PRIORITIZING URBAN AREAS FOR THE DEPLOYMENT OF HYPER-LOCAL FLOOD SENSORS USING STAKEHOLDER ELICITATION AND RISK ANALYSIS

Riccardo Negri[1], Luis Ceferino[2], and Gemma Cremen[3]

[1]PhD Candidate in Urban Systems, Civil and Urban Engineering Department, New York University. Email: r.negri@nyu.edu

[2]Civil and Environmental Engineering, University of California, Berkeley

[3]Civil, Environmental, and Geomatic Engineering Department, University College London

ABSTRACT

New urban monitoring networks with low-cost sensors can measure hyper-local floods in real-time in hundreds of locations. These novel networks promise enhanced flood risk management, especially within cities where floods can be extremely local. However, current sensor deployment strategies rely on limited metrics (e.g., proximity to densely populated areas) and do not adequately account for the various potential monitoring uses and stakeholders (e.g., emergency responders, critical infrastructure managers, and researchers). Thus, cities have no methodological framework to compare the holistic benefits of deploying new hyper-local sensors in different areas. To address this gap, we develop a framework to prioritize urban areas for sensor deployment based on potential uses for enhanced flood risk management and the exposure of infrastructure and community to high flood hazards at micro-urban scales. This framework includes (1) obtaining stakeholder feedback on the potential uses of sensors and relevant metrics for decision-making on their deployment, (2) quantifying these metrics with publicly available data to integrate them with flood hazard information through probabilistic risk analysis, and (3) combining the metrics to identify areas to be prioritized for sensor deployment. We tested the framework with a case study in New York City,

a densely populated urban area with highly heterogeneous communities and infrastructure exposed to high flood hazards. Through elicitation with 45 local stakeholders, we identified 32 potential uses and 58 metrics to prioritize areas for sensor deployment covering flood risk management, the welfare of residents, and the protection of critical infrastructure (e.g., transportation, drainage, and energy). Overall, the proposed framework and case study offer new insights into how modern monitoring networks can help to enhance flood disaster risk management in cities.

INTRODUCTION

Rapid urbanization and the changing climate have exacerbated flooding for many cities (Davenport et al. 2021). For example, in 2021 alone, New York City experienced two unprecedented flooding events that paralyzed the city, inundating numerous subway stations and killing 13 people (Plumer 2021; Newman 2021): on September 1st, Hurricane Ida delivered 3.15 inches of rain within an hour, surpassing the prior record of 1.94 inches set by Tropical Storm Henri only ten days before.

Flood monitoring is crucial for flood risk mapping, flood model validation, and flood damage assessment activities in cities (School 2018; Sarchani et al. 2020; Chen et al. 2021). Traditional approaches for recording flood hazards include stream gauges and field inspections for watermarks (Sarchani et al. 2020). However, these methods lack the scalability and accuracy to monitor urban floods effectively. For example, stream gauges are designed for use along river lines rather than inland areas within cities (Krabbenhoft et al. 2022). Watermarks indicate maximum flood depths and can sometimes be taken within cities, but the locations where such (often inaccurate) marks are preserved are extremely limited (Gardner et al. 2023).

Modern techniques for flood monitoring can significantly improve the coverage of urban flood measurements. For instance, remote sensing networks, which use satellite sensors, can provide measurements for entire cities with a resolution of less than 10 meters (Chawla et al. 2020). Due to their large coverage, these networks have been successfully used for monitoring hydrologic parameters in coastal cities and evaluating the impact of urbanization on flood risk (Bhatt and Srinivasa Rao 2018; Munawar et al. 2022). However, the high spatial resolution of these networks is offset by a relatively low temporal resolution of approximately one day in the best cases (Chawla et al. 2020), which precludes them from capturing severe, short-duration floods that often occur in cities (Alipour et al. 2020). In addition, the accuracy of remote sensing in dense cities can be affected by buildings that obstruct satellite measurements of the ground (Mason et al. 2012; Giustarini et al. 2013).

An emerging flood monitoring technique offers opportunities to address the shortcomings of remote sensing in cities. These networks consist of multiple low-cost sensors installed throughout city streets and sidewalks to measure floods in real-time at large urban scales (Figure 1). Examples of such "urban flood monitoring networks" include FloodNet in New York City (NYC) and StormSense in Hampton Roads, Virginia (Loftis et al. 2018; Silverman et al. 2022; Mydlarz et al. 2024). FloodNet presently operates ~ 85 sensors in NYC; this number will reach 500 by 2027 as part of a $7.2 million project funded by the city to increase climate resilience (Waraich 2023). These sensors measure water depth with ±5mm precision at one-minute intervals. During Hurricanes Henri and Ida in 2021, the sensors recorded remarkably rapid changes in water depths of almost three feet in less than an hour; see Figure 1 (FloodNet 2024). However, urban flood monitoring networks are limited in spatial coverage compared to remote sensing, as floods are only measured at locations where sensors are deployed. Thus, they require cities to develop a strategy for deploying (a limited set of) sensors that maximize network effectiveness in flood risk management.

Methods to evaluate sensor placement for collecting data on natural hazards have either focused on a single criterion such as hazard intensity (Krause et al. 2008; Wu et al. 2012; Du et al. 2014; Chang et al. 2019; Yu et al. 2022) or adopted multiple metrics that capture a broader representation of risk, like proximity to critical infrastructure and social vulnerability (Sun et al. 2018; Sun et al. 2019; Tien et al. 2023). These methods have two main limitations: (1) they fail to account for multiple potential users and uses of a monitoring network (e.g., government agencies for monitoring critical infrastructure, researchers for improving knowledge of hyper-local hazards, the general public for receiving real-time hazard alerts, etc.); and (2) their analysis is not explicitly informed by formal risk quantification, which requires combining spatial information on hazard

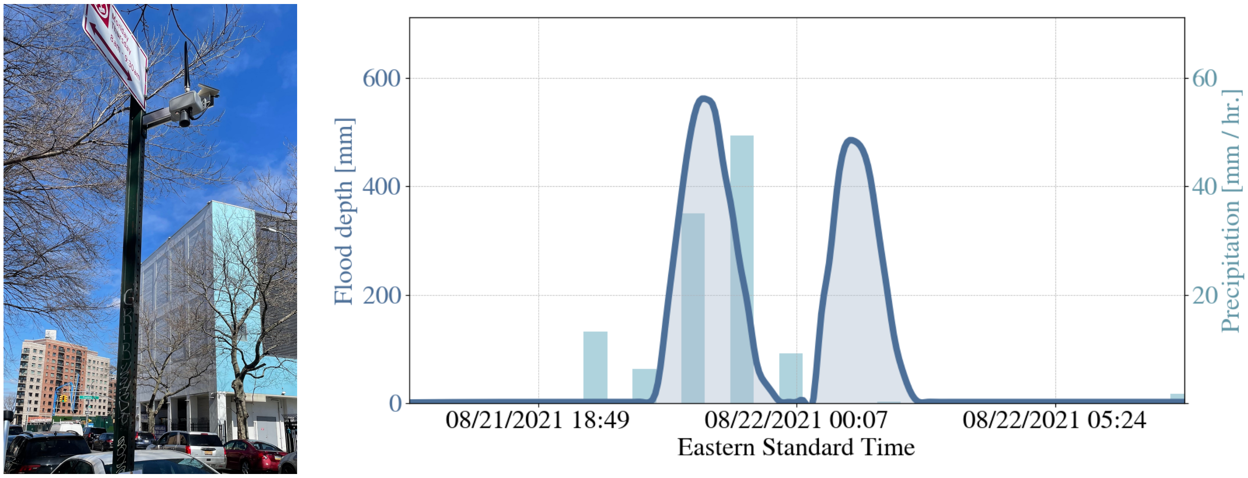

Fig. 1. A depiction of a typical FloodNet sensor (left) alongside sample data (right) demonstrating typical sensor performance during a flooding event. The lead author took the sensor picture from NYC streets. The picture does not imply that NYC officers or the FloodNet project endorse this study's results.

with metrics related to exposure and vulnerability.

We propose a framework for decision-making on low-cost sensor deployment in urban flood monitoring networks that addresses these two gaps. First, our framework identifies potential stakeholders of the monitoring network, to determine a comprehensive list of its various uses and establish a corresponding set of suitable metrics for evaluating potential sensor locations. Second, the framework integrates these metrics with flood hazard information in a probabilistic risk analysis to determine the likelihood and severity of flood impacts (e.g., expected annual number of flooded hospitals) across different urban areas. The result is a novel risk-informed, stakeholder-oriented spatial mapping of areas that should be prioritized for sensor deployment.

FRAMEWORK TO PRIORITIZE URBAN AREAS FOR SENSOR DEPLOYMENT

The proposed framework, outlined in Figure 2, comprises three stages. The first stage involves stakeholder elicitation to explore potential uses of the network and identify suitable metrics for evaluating sensor locations in terms of these uses. The second stage involves a flood risk analysis that combines the identified metrics with flood hazard models, enabling sensor deployment locations to be considered in the context of possible flood impacts. Stage three evaluates trade-offs between the metrics to investigate how the sensors can best be deployed to serve their multiple potential

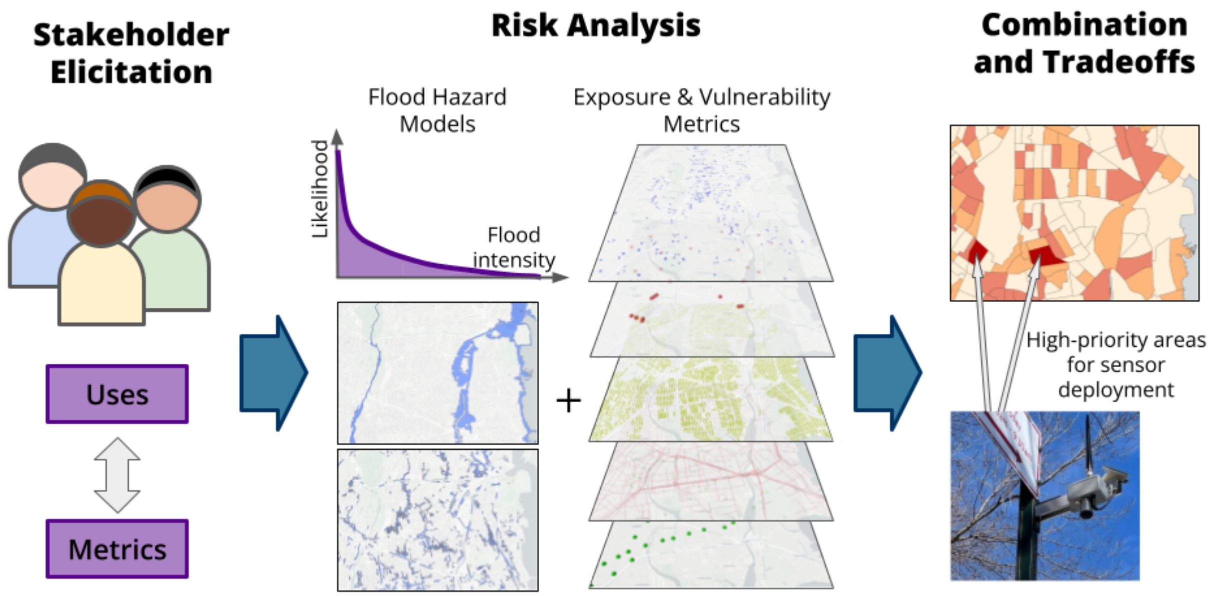

Fig. 2. Overview of the three-stage framework to prioritize flood sensor deployment areas through stakeholder elicitation, risk analysis, and metric combination and tradeoff analysis.

uses.

Stage 1: Stakeholder Elicitation

Stakeholder elicitation is an established method to systematically gather inputs and perspectives from relevant parties affected by a specific issue or project (Reed 2008). This stage of the framework has three main goals: (1) identify various flood risk management uses for the data generated by the monitoring network, (2) define a set of corresponding metrics that can be used to evaluate sensor locations according to these uses, and (3) include specific metrics that focus on particularly vulnerable communities with lower capacity to cope and recover from flooding disasters, e.g., because of lower income (Dow and Cutter 2006; Flanagan et al. 2011). The stakeholder elicitation stage occurs in three phases:

Stakeholder Identification

We followed the principles of stakeholder analysis to define a two-step process for determining relevant stakeholders (Gilmour and Beilin 2007; Pouloudi and Whitley 1997). The first step involves brainstorming a preliminary list of uses to identify an initial set of stakeholders. These stakeholders are then consulted to determine further potential uses and associated stakeholders.

We identified four key stakeholder categories from the literature on disaster risk management and hazard monitoring (Mojtahedi and Oo 2017; Rabinovici et al. 2022; Mojtahedi and Oo 2017; Fontainha et al. 2017; Cremen and Galasso 2021; Cremen et al. 2022; Webster et al. 2022): *government agencies, research institutions, the private sector, and resident representatives*. The last category refers to individuals who could speak or act on behalf of their community. While non-exhaustive, these stakeholder categories are key in risk management processes for natural hazards (Scolobig et al. 2014). These categories, which can be further refined into sub-categories or specific entities, can be used to determine the preliminary list of stakeholders.

Elicitation of Uses and Metrics

Next, stakeholder feedback is collected through the following three overarching questions:

1. "How and when would you use flood sensor data to help you in your duties before, during, or after floods?"

2. "What metrics could help prioritize the location of flood sensors according to your needs?"

3. "What social vulnerability metrics and related factors should also be considered when deciding on flood sensor placements?"

The stakeholder elicitation process must follow established guidelines (Chambers 2002; Department for International Development 2002; International Association for Public Participation 2004; Reed 2008; Knol et al. 2010; Wates 2014; Hemming et al. 2018; Rabinovici et al. 2022). For example, the workshops should be conducted in person where possible, to promote an effective exchange of ideas and foster discussion among participants (Rabinovici et al. 2022). The number of participants should be limited to 40-50 to allow enough time for everyone to share their views. Participants can further be divided into smaller working groups (e.g., ~ five people (Chambers 2002)) to promote richer discussions and interactions (Wates 2014). Workshops must be guided by moderators who clearly explain the workshop's goals and format and record the outputs of discussions using a visible medium (e.g., a whiteboard).

Following Rabinovici et al. (2022), stakeholders should spend 5 to 10 minutes independently formulating their responses to each question, which are then shared with the wider (working) group to develop a set of collective insights. These insights are used to define interim sets of *Use-Case Metrics*, (addressing question two) and *Social Vulnerability Metrics* (addressing question three). An example of a Use-Case Metric could be the volume of vehicular traffic on roads and highways, corresponding to the use of sensors in helping a local transportation department monitor traffic during flooding. An example of a Social Vulnerability Metric could be the income to indicate neighborhoods with low resources and likely disproportionately impacted by floods (Lee et al. 2022; Sanders et al. 2023).

The stakeholder analysis literature suggests that convening *resident representatives* and *government agencies* together in a single workshop could lead to more reserved and less open discussions, due to competing expectations and demands (Gilmour and Beilin 2007; Yu and Leung 2018; Blázquez et al. 2021). For example, *government agencies* might fear upsetting *resident representatives*, potentially leading to political repercussions. It is therefore recommended that the elicitation workshops are conducted in two rounds: (1) an initial round consisting of one workshop for *resident representatives* and another for the remaining stakeholder categories, and (2) a second combined workshop that is used to finalise the set of metrics, reflecting diverse perspectives. In the second combined workshop, stakeholder categories should be equally represented regarding participants to ensure a balanced outcome (Knol et al. 2010).

Selection of the Final Set of Prioritization Metrics

The interim sets of Use-Case Metrics and Social Vulnerability Metrics are refined by requiring each participant to select the three most important metrics from each set. These choices are indicated on visible media, e.g., using voting dots on a whiteboard. The n metrics chosen the most from each set are used for further analysis. We define the vector $\boldsymbol{v} \in \mathbb{R}^m$ to contain these m metrics. Thus, $m = 2 \cdot n$ for n Use-Case Metrics and n Social Vulnerability Metrics. By selecting a larger m, the sensor location decision-making process accounts for a wider range of network uses and a broader representation of social vulnerability. However, very large m values could cause problems in a subsequent post-processing activity, as explained in a following section. Finally, each stakeholder assigns an importance coefficient (α_j) to each of the m metrics in both sets, in line with their preferences on sensor deployment. The methodology for defining these coefficients is detailed in stage three.

Stage 2: Risk Analysis

This stage combines the metrics output from the previous stage with flood hazard models that account for different flood types and scenarios, using a probabilistic disaster risk analysis approach (Arora and Ceferino 2023b; Arora and Ceferino 2023a; Avraam et al. 2023; Arora and Ceferino 2024). The results are spatialized sets of sensor deployment prioritization measurements that account for flood intensity (i.e., risk values). The stage includes four steps:

Definition of Geographic Units

The region of interest $\mathcal{A}$ is subdivided into smaller geographic units $\mathcal{P} = \{A_i \mid i = 1, \ldots, t\}$, where t is the number of geographic units that compose the city. $\mathcal{A} = \cup_{i=1}^{t} A_i$ and $A_i \cap A_j = \emptyset, \forall i \neq j$, i.e., A_i are collectively exhaustive and do not overlap. Each A_i represents one spatial point in the risk analysis process and is therefore associated with unique measurements of sensor deployment prioritization (risk values). The number of sensors deployed in each geographic unit depends on the total number of available sensors N compared to t. If $N < t$, a single sensor could be deployed in each N A_i with the highest priority (measured using the $I(A_i)$ index introduced later). If $N > t$, more sensors could be deployed in higher priority units than those with less importance.

The size of A_i is constrained by two factors. The first is the availability and granularity of data for each considered metric. Cities may have key urban information recorded at various scales, ranging from city blocks to larger administrative boundaries (City of New York 2023; City of San Francisco 2023). The second is the level of spatial correlation in flood intensity between flood-prone areas; if this is too high between units, there may be redundant locations where sensors would record the same information. We can decrease redundancies through methods that maximize hazard information as long as sufficient relevant information is available (Krause et al. 2008; Wu et al. 2012; Du et al. 2014; Chang et al. 2019; Yu et al. 2022). Without this information, decisions on the size of A_i in terms of minimizing redundancies can only be judged mainly qualitatively from available flood data.

Definition of Flood Hazards

The flood hazard data can represent multiple flood types affecting a city, e.g., storm surge, pluvial, riverine, and tidal flooding. For each considered flood type w, we can have different spatialized intensity maps (e.g., with flood depths spatial extents) associated with a corresponding return period $T \in \mathbb{R}^+$, i.e., the average time interval between occurrences of a flood associated with given intensities or larger. Each intensity map for a specific flood type can constitute a flood scenario.

To represent a flood scenario, we define a function $g(T)$ that maps a return period T to a flooded geographic area $\mathcal{F}$. For each flood type w, the function g_w is formally defined as $g_w : \mathbb{R}^+ \rightarrow \mathcal{F}$, where $\mathcal{F}$ represents the set of all flooded areas composed of polygons enclosing affected geographical extents. Figure 3 illustrates the interaction between A_i and $g_w(T)$ for $T = T_1$ and $T = T_1 > T_2$ for a generic flood type w. Note that the area covered $g(T)$ is monotonically increasing, as flood-prone areas identified by $\mathcal{F}$ can only remain constant or expand for growing T.

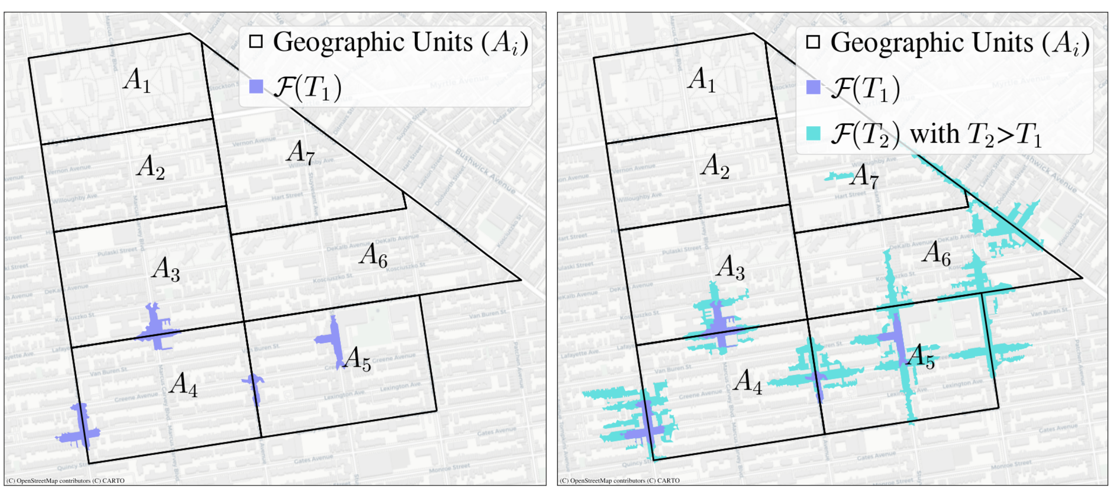

Fig. 3. Example partition of a city into geographic units, denoted as (A_i), and illustration of the function $g_w(T)$ that represents the spatial extent of flooding for varying return periods and a generic flood type w.

For each geographic unit $A_i \in \mathcal{P}$ and each considered flood type w, we then define a Bernoulli random variable $B_w(A_i)$ representing whether a flood occurs or not any given year for the considered flood type w. $B_w(A_i)$ can take a value of 1 with probability $p(A_i \cap g_w(T) \neq \emptyset)$, i.e., the probability that the geographic unit intersects with the flood scenario with return period T, or 0 with probability $1 - p(A_i \cap g_w(T) \neq \emptyset)$. Under Poisson assumptions,

$$p(A_i \cap g_w(T) \neq \emptyset) = 1 - e^{-1/T_w^*(A_i)}, \tag{1}$$

where $T_w^*(A_i) = \min\{T \mid A_i \cap g_w(T) \neq \emptyset\}$. In other words, $T_w^*(A_i)$ is the minimum return period for which A_i experiences flooding for flood type w. $T_w^*(A_i)$ is determined by investigating the set of flood scenario data of flood type w available for the city of interest; these data are now accessible for many geographic regions and multiple return periods (Wing et al. 2023).

While $T \in \mathbb{R}^+$ is continuous, often flood hazard data may be only available for a few return periods. In that case, we can still use the same formulation presented in this paper. For example, if only maps for two return periods are available, like in Figure 3, the function $g_w(T)$ can be defined as follows:

$$g_w(T) = \begin{cases} \emptyset & \text{for } 0 \leq T < T_1, \\ \mathcal{F}(T_1) & \text{for } T_1 \leq T < T_2, \\ \mathcal{F}(T_2) & \text{for } T \geq T_2. \end{cases} \tag{2}$$

For A_3, A_4 and A_5, the minimum return period causing flooding is T_1 (i.e., $T_w^*(A_3) = T_w^*(A_4) = T_w^*(A_5) = T_1$). A_6 and A_7 start becoming flooded for T_2 (i.e., $T_w^*(A_6) = T_w^*(A_7) = T_2$). A_1 and A_2 do not experience flooding at T_2 (i.e., $T_w^*(A_1) = T_w^*(A_2) = +\infty$ in the absence of additional flood scenarios with $T > T_2$).

Characterization of Metrics

Given $\boldsymbol{v} \in \mathbb{R}^m$ (output from the stakeholder elicitation stage), we define a corresponding vector $\boldsymbol{v}(A_i)$ that represents values of the m metrics for each A_i. Note that $v_j(A_i)$ values for Social Vulnerability Metrics are scaled by the number of residents living in A_i to also account for exposure.

Quantifying Risk

This step computes an expected annual value $\boldsymbol{V}(A_i)$ corresponding to $\boldsymbol{v}(A_i)$. Considering a specific flood type w, the expected annual value $\boldsymbol{V}_w(A_i)$ is calculated as follows:

$$\boldsymbol{V}_w(A_i) = \mathbb{E}[\boldsymbol{v}(A_i) \cdot B_w(A_i)] = \boldsymbol{v}(A_i) \cdot \left(1 - e^{-1/T^*_w(A_i)}\right) \tag{3}$$

We consider multiple flood types independent and that damage from multiple floods is cumulative. Thus, the expected value of the sum of the effects of each flood type is the sum of the individual expected values:

$$\boldsymbol{V}(A_i) = \mathbb{E}\left[\sum_w (\boldsymbol{v}(A_i) \cdot B_w(A_i))\right] = \boldsymbol{v}(A_i) \cdot \sum_w \left(1 - e^{-1/T^*_w(A_i)}\right) \tag{4}$$

For example, consider a hypothetical metric v_1 (e.g., “Number of residential buildings”). Assume that the geographic unit A_i contains 100 such buildings (i.e., $v_1(A_i) = 100$), and the minimum return periods causing flooding in A_i are $T^* = 100$ years for flood type 1 (e.g., storm surge), and $T^* = 10$ years for flood type 2 (e.g., riverine). The expected annual number of at-risk residential buildings in A_i, $V_1(A_i)$, is then computed as:

$$V_1(A_i) = 100 \cdot \left[\left(1 - e^{-1/100}\right) + \left(1 - e^{-1/10}\right)\right] = 10.5$$

Stage 3: Combination of Metrics and Tradeoffs Between Deployment Areas

Metrics are considered simultaneously by combining them into a unique index $I(A_i)$ that is calculated in two steps. The first involves defining the α_j importance coefficients at the end of the stakeholder elicitation process. These coefficients are then used to scale normalised versions of each metric and the results are linearly combined to produce $I(A_i)$.

Quantifying the Relative Importance of Different Metrics

The importance coefficients are determined using the Analytical Hierarchy Process (AHP) (Saaty 1987). This process is chosen for its ability to systematically decompose complex problems into manageable sub-problems and its consistency-check mechanism that ensures the reliability of decision-maker judgments. Importance coefficients for Use-Case Metrics and Social Vulnerability Metrics are defined separately because each set has different objectives. Use-case metrics center on the practical purposes of sensor data for different stakeholders (e.g., monitoring infrastructure, enhancing flood understanding, whereas Social Vulnerability Metrics focus on vulnerable populations.

AHP consists of pairwise comparisons of metric h against k, assigning a score from one to nine to indicate their relative importance. A score of one means both metrics are equally important. A score of two for metric h suggests it is slightly more important than k, while a score of nine indicates a significant importance difference. Scores between these values represent varying levels of relative importance. The AHP scores are assigned to a matrix, where cell h, k indicates the relative importance of metric h compared to k, and cell k, h stores the reciprocal value. According to the established AHP methodology, this matrix's principal eigenvector components provide the α_j importance coefficients assigned to each metric (Saaty 1987). Note that AHP decreases in reliability when the number of considered metrics exceeds approximately 7 to 9 (Saaty 1987), which constrains the value of m.

Each participant (stakeholder) performs AHP individually, using printed tables or software. Individual AHP matrices are assessed using the Consistency Ratio (CR), an index that evaluates the coherence of the pairwise comparisons. Only matrices with a CR of less than 0.10 are retained according to the recommendations outlined in (Saaty 1987). α_j for each metric is then quantified as the geometric mean of the corresponding principal eigenvector component associated with each valid matrix.

We denote as $\boldsymbol{\alpha} \in \mathbb{R}^m$ the vector containing the importance coefficients associated with each metric in $\boldsymbol{v}(A_i)$. The first n entries of $\boldsymbol{\alpha}$ represent importance coefficients for the Use-Case Metrics, and the remaining n entries denote the importance coefficients for the Social Vulnerability Metrics.

Combining Metrics into a Unique Index

The metrics are first normalized to a comparable scale because they are typically expressed in various units, e.g., annual average daily traffic on roads, and number of subway stations. Normalization methods that can be employed include Percentile normalization (transforming metric values to percentiles), Min-max scaling (rescaling data to a 0–1 range), and Standardization (modifying data to achieve a mean of 0 and a standard deviation of 1) (Saisana et al. 2005). We then calculate $V_a(A_i)$ and $V_b(A_i)$ as

$$V_a(A_i) = \sum_{j=1}^{n} \overline{V}_j(A_i) \cdot \alpha_j \tag{5}$$

$$V_b(A_i) = \sum_{j=n+1}^{m} \overline{V}_j(A_i) \cdot \alpha_j \tag{6}$$

where a corresponds to the Use-Case Metrics, b corresponds to the Social Vulnerability Metrics and $\overline{V}_j(A_i)$ denotes normalized values. Then:

$$I(A_i) = \gamma \cdot V_a + (1 - \gamma) \cdot V_b \tag{7}$$

where $\gamma \in [0, 1]$ represents the relative importance of Use-Case Metrics over Social Vulnerability Metrics (such that $\gamma = 0.5$ denotes equal importance). γ could also be determined through stakeholder elicitation.

A_i with the highest $I(A_i)$ values should be prioritized in terms of sensor deployment. The precise placement of sensors within each A_i can be based on the individual metrics contributing more to $I(A_i)$, e.g., close to critical infrastructure if this metric contributes substantially. Ideally, high $I(A_i)$ values should be sense-checked against any available ground-truth data (e.g., field survey, satellite imagery) to ensure they adequately reflect actual flood risk conditions.

CASE STUDY IN NEW YORK CITY

We chose NYC as a proof-of-concept case study of the proposed framework for four main reasons. First, NYC provides abundant publicly accessible data for implementing the proposed framework. Second, the city faces significant flood risks due to its densely populated nature, vulnerable infrastructure, and heterogeneous social groups. Third, NYC has several initiatives for reducing flood impacts, including the FloodNet urban flood monitoring network. Our case study focuses on deploying these sensors in the city, but we want to note that the actual sensor deployment strategy of FloodNet differs from what is presented in this paper. Fourth, many authors of this paper are or were based in NYC and could, therefore, leverage local connections to recruit stakeholders for this study.

Stage 1: Stakeholder Elicitation

Stakeholder Identification and Elicitation Process Set Up

The stakeholder elicitation process consisted of a single workshop involving the following stakeholder categories: *government agencies, research institutions, and the private sector*. We classified government agencies into two primary categories: those engaged in emergency response (e.g., the Fire Department) and those overseeing various public services and infrastructure. In terms of the latter, we distinguished between agencies responsible for infrastructure directly related to flood risk mitigation (e.g., the Department of Environmental Protection) and those managing other types of infrastructure (public services) that could potentially be impacted by natural hazards (e.g., the Departments of Transportation, Parks, Housing, Sanitation, Education). Research institutions were divided into two sub-categories: (1) academic research institutions consisting of universities; and (2) non-academic research institutions that include governmental research institutions specializing in flood studies (e.g., the National Oceanic and Atmospheric Administration), community-based initiatives on flood data collection (e.g., the Community Flood Watch Project (com 2023)), and private entities focused on flood risk assessment and modeling (e.g., the First Street Foundation (fir 2023)). We included private sector stakeholders through catastrophe (re)insurance companies and civil engineering consultancies engaged in flood mitigation.

The refined stakeholder classifications were used to recruit stakeholders for the workshop. Potential participants were targeted from the authors' network and were contacted three months before the event. We extended workshop invitations to 74 stakeholders that represented each

TABLE 1. Information on participants involved in the stakeholder elicitation process .

Category	Number	Subcategory	Number
Government agencies	16 (37%)	Emergency response	25%
		Non-emergency response	75%
Research institutions	23 (50%)	Academic	90%
		Non-academic	10%
Private sector	6 (13%)	Insurance	67%
		Civil Engineering consultants	33%

stakeholder category in the following proportions: 43% (research institutions), 41% (government agencies), and 16% (private sector). Given the proof-of-concept nature of the case study, our priority was to maximize stakeholder participation rather than to achieve a balanced representation of stakeholder categories. 45 stakeholders ultimately participated in the workshop; their distribution across stakeholder categories is detailed in Table 1.

The workshop was held at the New York University in a conference room with 8-chair tables, whiteboards, and a large screen. Groups, each with six to seven stakeholders randomly mixed together in terms of stakeholder category, were arranged at eight tables. Adhesive voting dots were provided for the voting activity required to select the final prioritization metrics. Paper tables were used to facilitate the pairwise comparisons of the AHP process. Note that stakeholders did not discuss how metrics could be quantified during the workshop (e.g., in terms of absolute numbers or percentages) or consider data availability. These issues were addressed in stage two (risk analysis).

Answers to Question #1: How and when would you use the flood sensor data to help you in your duties before, during, or after floods?

Thirty-two potential uses of sensor data were discussed. These uses can be broadly categorized as follows: (1) emergency response and recovery planning; (2) infrastructure and public service management; (3) flood risk awareness; and (4) improving the characterization of flood hazard and risk. (See Supplementary Information for a complete list of the 32 uses, organized by category). For example, regarding the first category, it was identified that sensor data could be used during the emergency phase to direct rescue and relief operations to the most affected areas, ensuring timely and effective aid. Sensor data could also be used in the post-event recovery period as a proxy for assessing damage and informing strategic resource allocation for cleanup, repairs, and community support.

For the second category, it was identified that sensor data could be used to evaluate the effectiveness of green infrastructure projects by monitoring the rate at which they absorb or redirect rainfall or assess the performance of stormwater systems by measuring flow and capacity during various weather conditions, for example. The data could also pinpoint flood-prone areas as part of infrastructure planning activities, guiding flood defense investment decisions. Furthermore, sensor data could be useful for managing infrastructure unrelated to flood mitigation. The data could help inform decision-making (e.g., prompt preemptive shutdowns or flood barriers) for essential facilities, such as wastewater and energy infrastructure, public services (e.g., garbage collection, snow-plowing, education), and transportation (e.g., bus services, metro stations) affected by flooding.

Concerning the third category, dissemination of sensor data through various channels (e.g., media, in-person education workshops, reports, etc.) could play an important role in conveying the extent of previous local floods to residents, increasing their awareness of flood risk. Residents could use sensor data as evidence of flooding to support applications for post-storm financial assistance, receive financial aid for building upgrades related to flood-risk mitigation, and advocate for receiving public funding for flood-risk protection and mitigation infrastructure.

As for the fourth category, sensor data could be used to empirically refine the parameters of hydrologic and hydraulic models (e.g., the catchment runoff coefficient, soil permeability and infiltration rates, drainage system capacity), and quantify spatial and temporal correlations in flood intensities. Information on past floods could also help property buyers to more rigorously account for flood risk when assessing real estate values (Rajapaksa et al. 2016). Private insurers and government agencies involved in flood risk assessment and insurance provisioning (e.g., the Federal Emergency Management Agency in the US) could use sensor data to identify insurance gaps related to flood protection (e.g., determine neighborhoods with flood exposure but no flood insurance, or where flood risk is underestimated). Sensor data can also be used by insurers as a trigger for parametric insurance policies (Lin and Kwon 2020), which provide payouts based on the occurrence of predefined conditions related to an event, such as the exceedance of a certain flood depth.

Answers to Question #2: 'What metrics could help prioritize the location of flood sensors according to your needs?"

Workshop participants identified 23 Use-Case Metrics in Question 2 (See Supplementary Information for a full list). Some metrics relate to more than one of the use cases determined in response to Question 1. For instance, "Number of basement dwellings" could correspond to the use of sensor data in either helping emergency responders direct rescue operations toward areas with a higher prevalence of such dwellings or raising flood awareness for residents living in these dwellings. Several metrics focus on using sensor data for infrastructure management, e.g., "Number of flood mitigation infrastructure projects" and "Number of critical infrastructure facilities". Metrics related to raising flood awareness include "Number of buildings without flood insurance". Metrics associated with enhancing the characterization of flood hazard include "Number of citizen-reported flood incidents" and"Number of applications for post-flood assistance". These metrics could help identify flood-prone areas in the absence of flood models. They could also be used to benchmark and, therefore, improve the accuracy of flood models, where available (Negri et al. 2023).

Answers to Question #3: "What social vulnerability metrics and factors should be considered when deciding on flood sensor placements?"

Workshop participants identified 35 Social Vulnerability Metrics in addressing Question 3 (see Supplementary Information for a full list of these metrics). Three of the identified metrics are well-established indices. The most well-known one is the Social Vulnerability Index (SVI), which assesses the resilience of communities under external stresses, such as disasters or other emergencies. Several versions of SVI exist in the literature, such as the Centers for Disease Control and Prevention / Agency for Toxic Substances and Disease Registry's (CDC/ATSDR) SVI (Flanagan et al. 2011), and the SVI developed by (Dow and Cutter 2006). The other two indices

TABLE 2. The eight Use-Case Metrics that received the highest number of votes

METRIC NUMBER	METRIC DESCRIPTION
v_1	Number of critical infrastructure facilities (e.g., energy, communications, wastewater facilities)
v_2	Number of buildings not compliant with updated building code regulations
v_3	Vehicular and foot traffic along (private and public) transportation routes
v_4	Level of uncertainty in flood model predictions (e.g., mismatch between flood reports and modeled flooding)
v_5	Number of bus and subway stations
v_6	Number of flood mitigation infrastructure projects (e.g., green infrastructure)
v_7	Number of polluted sites (e.g., brownfield land)
v_8	Historical number of flood insurance claims

identified are the Environmental Protection Agency's Environmental Justice Index (EJI) ((EPA) 2023) and the NYC Displacement Risk Index (NYCDCP 2023). EJI assesses the environmental burden and vulnerability of communities, focusing on exposure to pollutants and health risks. The NYC Displacement Risk Index evaluates the risk of residents being involuntarily displaced due to rising housing costs, eviction, or redevelopment.

The complete set of identified Social Vulnerability Metrics was subsequently organised into four categories: (1) Socio-economic and Demographic factors, (2) Access to Public Services and Infrastructure, (3) Community Engagement, and (4) Risks from Compounding Hazards., which align with those identified in previous studies on social vulnerability and natural hazards (Cutter et al. 2010; Finch et al. 2010; Dow and Cutter 2006; Garbutt et al. 2015; Daniel et al. 2022; Englund et al. 2023).

Selection of the Final Set of Prioritization Metrics

Workshop participants voted to determine the eight Use-Case Metrics and eight Social Vulnerability Metrics to be used for prioritization; see Tables 2 and 3 (i.e., $m = 16$).

TABLE 3. The eight Social Vulnerability Metrics that received the highest number of votes

METRIC NUMBER	METRIC DESCRIPTION
v_9	Social Vulnerability Index
v_{10}	Number of essential public services (e.g., schools, markets, evacuation centers) per capita
v_{11}	Level of compound risk (e.g., from flooding and heat)
v_{12}	Level of social isolation/civil capacity (e.g., number of senior or community centers per capita)
v_{13}	EPA Environmental Justice Index
v_{14}	Usage of the 311 (Wikipedia contributors 2023) reporting system by residents
v_{15}	Percentage of non-documented households
v_{16}	Median housing costs relative to median household income

Stage 2: Risk Analysis

Definition of Geographic Units

We examined the city at the census tract level for three main reasons. First, census tracts are defined to be relatively uniform with respect to population characteristics, economic status, and living conditions (United States Bureau of the Census 1994). Second, relevant data are available at this level of granularity.

Definition of Flood Hazards

NYC is exposed to three flood types: storm surge, pluvial flooding, and tidal flooding (Rosenzweig et al. 2013). Separate maps are available for each. The storm surge maps considered in this study are those developed by the New York City Panel on Climate Change (NPCC), which combine sea level rise projections with FEMA's 2013 Preliminary Work Maps for 100-year and 500-year return periods (Patrick et al. 2019). The pluvial maps considered are the NYC Stormwater Flood Maps (NYC Mayor's Office of Resiliency 2021), which depict rainfall-induced flood extents under current and future climate conditions for a moderate (10-year return period) and an extreme (100-year) rain event. The tidal flood maps considered are from NPCC (Patrick et al. 2019), which depict current high tide levels. Figure 4 presents two examined flood maps. Tidal flooding is

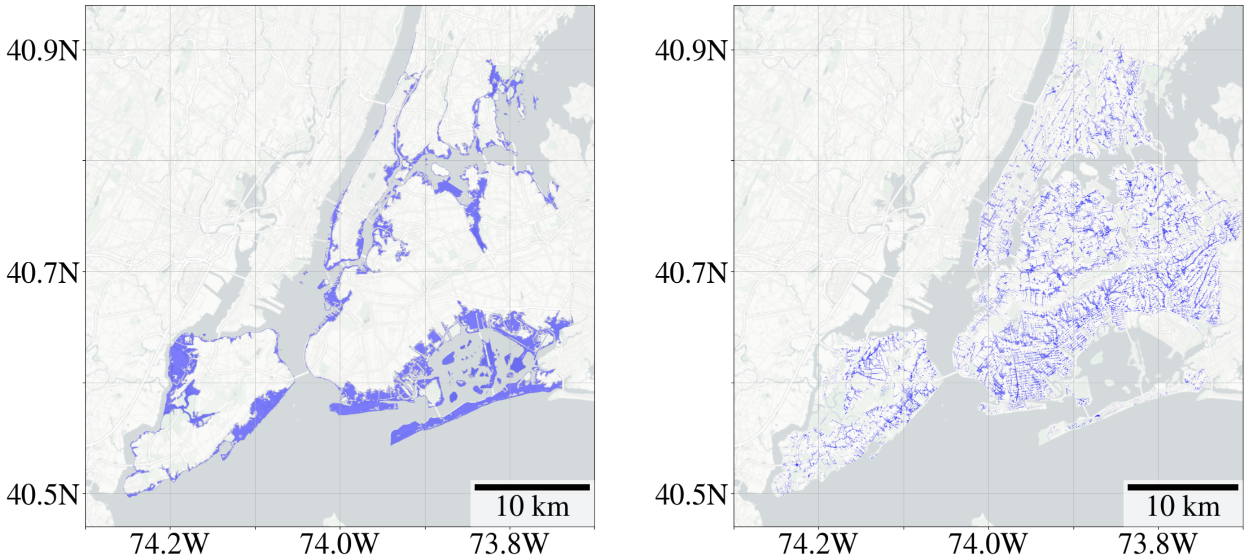

Fig. 4. Storm surge flood map (left) and pluvial flood map (right) for New York City, both corresponding to a return period of T = 100 years. The storm surge map shows areas flooded by sea water intrusion during a storm surge, typically along coastlines and river mouths. The pluvial flood map displays flooding from heavy rainfall accumulating on the land surface, which creates a dispersed pattern across the urban landscape.

assigned a probability of 1 for any given year, given the certainty of high tides occurring multiple times yearly.

Characterization of Metrics

The characterization process required some of the $m = 16$ metrics to be slightly refined or disregarded based on data availability and potential overlaps. Tables 4 and 5 describe the refined versions of metrics. The Supplementary Information provides the data sources, types, and the quantification method associated with characterized metrics.

Metrics v_4 and v_{14} required more elaborate refinement given their original broad definitions. These metrics were quantified based on the number of tax lots, which are individual parcels of land defined for property tax purposes (a Census tract contains, on average, 350 tax lots), and information on the number of 311 reports. The 311 reports and the tax lot data were then aggregated at the census tract level. More specific details on their characterization are provided in the next section.

TABLE 4. Characterized Use-Case Metrics

ORIGINAL METRIC	REFINED METRIC	EXPLANATION
v_1 – Number of critical infrastructure facilities (e.g., energy, communications, wastewater facilities)	Number of electricity substations	Electricity substations are examined due to their critical role in maintaining essential services and economic stability. Substations are particularly vulnerable to flooding, as observed during past events (New York City Government 2023), leading to widespread power outages affecting safety, health, and business activities. Sensor data can aid in the management of these facilities during emergencies, such as enabling preemptive shutdowns to mitigate damage.
v_2 – Number of buildings not compliant with updated building code regulations	Number of residential units in pre-1961 buildings	The NYC 1961 Zoning Resolution is selected as the building code of interest, due to its regulatory significance (NYP). Sensor data can help identify the buildings most impacted by flooding, facilitating targeted allocation of restoration resources.
v_3 – Vehicular and foot traffic along (private and public) transportation routes	Annual Average Daily Traffic (AADT) of vehicles along roads and highways	AADT is used due to the high volumes of vehicular movement in NYC. Sensor data can aid in managing the road network during flood events, for example, by optimizing rerouting strategies to prevent congestion.
v_4 – Level of uncertainty in flood model predictions	Discrepancy between flood maps and flood reports: Areas where flood reports exceed flood map predictions	Discrepancy between flood maps and reports is used to measure model uncertainty, highlighting areas where model predictions used to produce the flood maps do not match flood occurrences as measured by resident reports. The characterization of this metric is explained separately.
v_5 – Number of bus and subway stations	Annual Average Ridership (AAR) for subway stations	AAR for subway stations is used, given the significant damage experienced in subway stations during past flooding events like hurricanes Sandy and Ida. This metric focuses on stations where service disruptions would impact the largest number of passengers. Sensor data can help manage the subway network during flooding, for example, by facilitating the timely closure of flooded stations and rerouting of passengers.
v_6 – Number of flood mitigation infrastructure projects (e.g., green infrastructure)	Spatial extent of public green infrastructure projects	Green infrastructure projects are a key flood-mitigation initiative in NYC (Catalano de Sousa et al. 2016; Culligan 2019; Geberemariam 2017). Sensor data can assist in monitoring the effectiveness of green infrastructure projects, enabling performance evaluation for future planning.
v_7 – Number of polluted sites (e.g., brownfield lands)	Number of New York State (NYS) classified environmental remediation sites	NYS classifies all polluted sites in a geo-located database named Environmental Remediation Sites. Flooding can disperse pollutants, and sensor data can trigger targeted remediation efforts.
v_8 – Historical number of flood insurance claims	Proxy not included in the case study because of lack of data	N/A

TABLE 5. Characterized Social Vulnerability Metrics

ORIGINAL METRIC	**REFINED METRIC**	**EXPLANATION**
v_9 – Social Vulnerability Index	Social Vulnerability Index	No refinements required.
v_{10} – Number of essential public services (e.g., schools, markets, evacuation centers) per capita	Floor area of public schools per capita	Schools were specifically selected for examination, given that they often serve as emergency shelters (Long 2017), implying that areas with ample school space are better prepared for disasters.
v_{11} – Level of compound risk (e.g., from both flooding and heat)	No refined version of the metric is created due to data unavailability	N/A
v_{12} – Level of social isolation/civil capacity (e.g., number of senior or community centers per capita)	Number of human service centers per capita	Human service centers include community centers, employment centers, and senior centers. The presence of such services is deemed a reasonable proxy for civil capacity.
v_{13} – Environmental Justice Index	Environmental Justice Index	No refinements required.
v_{14} – Usage of the 311 reporting system by residents	Discrepancy between flood reports and flood maps: Areas where flood map predictions exceed flood reports	Discrepancy between flood map predictions, and actual flood reports are used to measure the underreporting of flood events, highlighting areas where fewer reports are filed despite high risk predicted by flood maps. The characterisation of this metric is explained separately.
v_{15} – Percentage of non-documented households	No refined metric version is created due to data unavailability.	N/A
v_{16} – Median housing costs relative to median household income	No refined version of the metric is created because it is already highly correlated with v_9.	N/A

Quantifying Risk

Given that data used for characterizing each metric are available at a finer resolution than the granularity of the selected A_i (i.e., census tracts), only spatial elements that intersect with inundation on each flood map were used to quantify $\boldsymbol{V}(A_i)$ (and count towards flood exposure) in this case study. For instance, take A_i as Census tract #1003300 in Downtown Manhattan. A_i contains two subway stations referred to as *Station A* and *Station B* (Figure 5). *Station A* and *Station B* record AAR of 5,415,350 passengers and 1,331,778 passengers, respectively. Both stations intersect with the 100-year storm surge map (Figures 5a and 5b). *Station A* intersects the 10-year pluvial flood map (see Figure 5c), whereas *Station B* only intersects the 100-year pluvial flood map (see Figure 5d). In the absence of tidal flooding, this means that $V_5(A_i)$ is computed as

$$\begin{aligned} V_5(A_i) = \mathrm{AAR}(StationA) \cdot \left(1 - e^{-1/10} + 1 - e^{-1/100}\right) + \\ + \mathrm{AAR}(StationB) \cdot \left(2 \times (1 - e^{-1/100})\right) = 595,725 \end{aligned} \tag{8}$$

v_4 and v_{14} were instead quantified as discrepancies between the expected annual number of tax lots exposed to flooding (y calculated analogously to equation 8) and the annual average number of flood-related 311 reports (x calculated using all available data from 2010 to the present) per A_i. A linear regression was performed for each pair of x and y to compute the slope coefficient m. The annual *predicted* number of flooded tax lots ($\hat{y}$) is then given by

$$\hat{y} = x \cdot m \tag{9}$$

$V_4(A_i)$ is then computed as

$$V_4(A_i) = \begin{cases} \frac{\hat{y}-y}{\hat{y}+1}, & \text{if } y \leq \hat{y} \\ 0, & \text{if } y > \hat{y} \end{cases} \tag{10}$$

$V_4(A_i)$ can be considered an indicator of flood hazard underestimation. The denominator in Equation 10 avoids that areas with many tax lots within flood-prone areas dominate the results. The unit constant in the denominator differentiates between tracts with a positive number of reports but

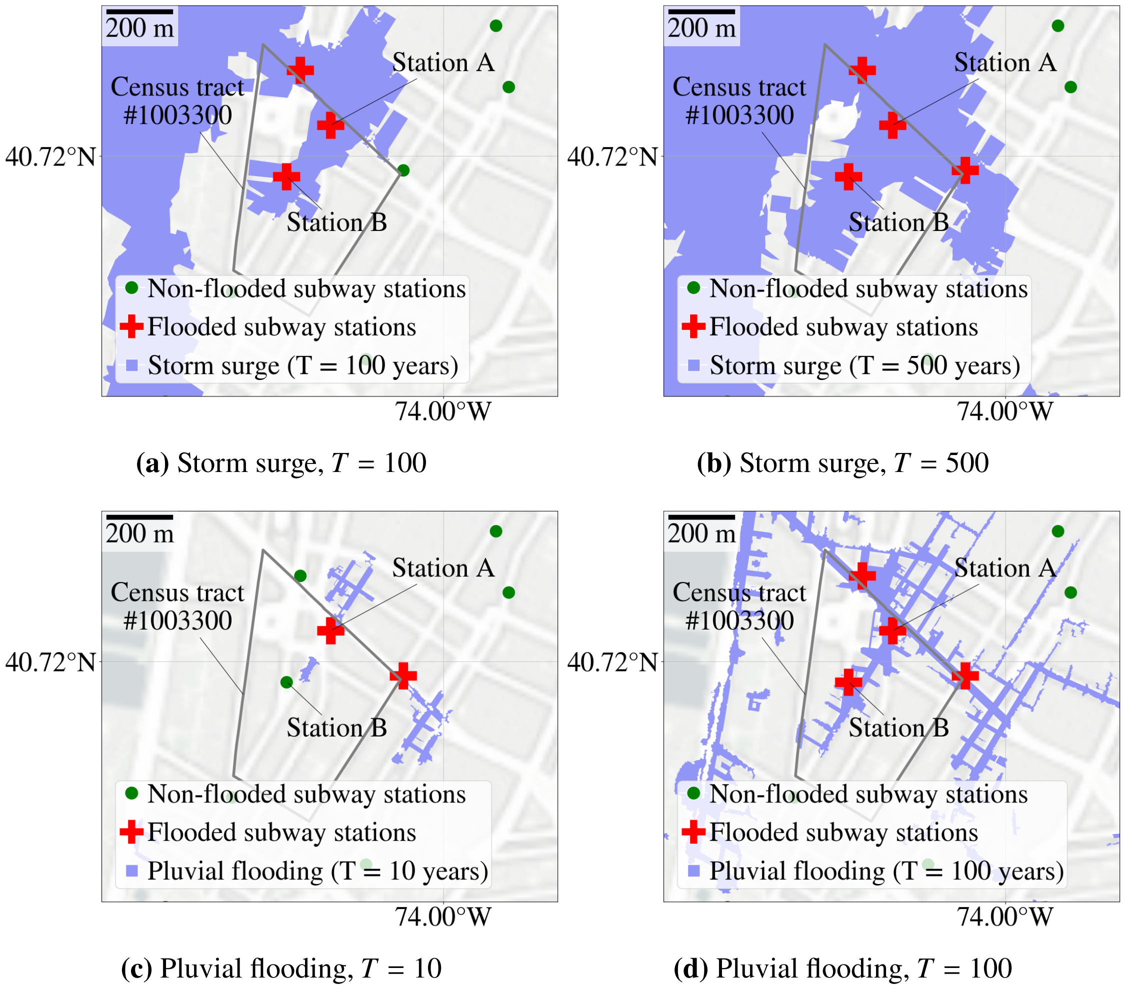

Fig. 5. Map of the NYC subway stations in Census tract #1003300 intersected with flood maps with different return periods.

no tax lots in flood-prone areas. By adding the unit constant, tracts with more reports are assigned higher V_4. $V_{14}(A_i)$ was calculated the same way as $V_4(A_i)$ except that x and y were inverted, such that $\hat{y} - y$ reflects the discrepancy between the number of 311 reports forecasted by the linear regression model and the actual number of recorded reports. Larger $V_{14}(A_i)$ may signal potential underutilization of the reporting system within the considered community.

Stage 3: Combination of Metrics and Tradeoffs Between Deployment Areas

The weights α_j obtained during the AHP process were rescaled to sum to one because of the dropped metrics. The final values of α_j are provided in the Supplementary Information.

TABLE 6. The three census tracts in each borough with the highest values of $I(A_i)$ and the corresponding metrics that rank within the top quartile.

Borough	Ref. on Figure 6	Overall ranking of I value	Top Quartile Metrics
Manhattan	A	41	v_2, v_6, v_9
	B	6	v_2, v_3, v_5, v_9, v_{10}
	C	44	v_3, v_4, v_9
Bronx	D	67	v_2, v_3, v_9
	E	20	v_9, v_{12}
	F	90	v_2, v_{10}, v_{12}
Queens	G	4	v_2, v_3, v_4, v_{10}, v_{12}
	H	1	v_2, v_3, v_9, v_{13}
	I	3	v_1, v_2, v_{12}, v_{13}, v_{14}
Brooklyn	J	13	v_2, v_3, v_{13}
	K	12	v_2, v_3, v_6, v_{14}
	L	5	v_2, v_7, v_{10}, v_{12}
Staten Island	M	28	v_2, v_3, v_6, v_{12}, v_{13}, v_{14}
	N	2	v_2, v_3, v_6, v_{13}
	O	8	v_2, v_3, v_{13}, v_{14}

Combining Metrics into a Unique Index

To compute $V_a(A_i)$ and $V_b(A_i)$ (Equations 5 and 6), each metric was normalized using percentile normalization. $I(A_i)$ was then calculated for $\gamma = 0.50$ (Figure 6). We assigned to γ the value of 0.50 because the relative importance of Use-Case Metrics and Social Vulnerability Metrics was not investigated during the stakeholder elicitation process.

We analysed individual metrics for the three census tracts in each NYC borough with the highest $I(A_i)$ (denoted using letters A to O in Figure 6), in terms of their quartile values. Table 6 provides the metrics that rank in the top quartile for each A_i.

Each metric features in at least one row of Table 6, demonstrating the effectiveness of I in collectively capturing the metrics. Multiple metrics rank in the top quartile for each A_i in Table 6, indicating compounding sources of risk. For example, Washington Heights in northern Manhattan, labeled ***B*** in Figure 6, which faces relatively frequent inundation from pluvial flooding and storm surge, is an important vehicular transport junction (annual AADT at risk of 3,000 vehicles), a

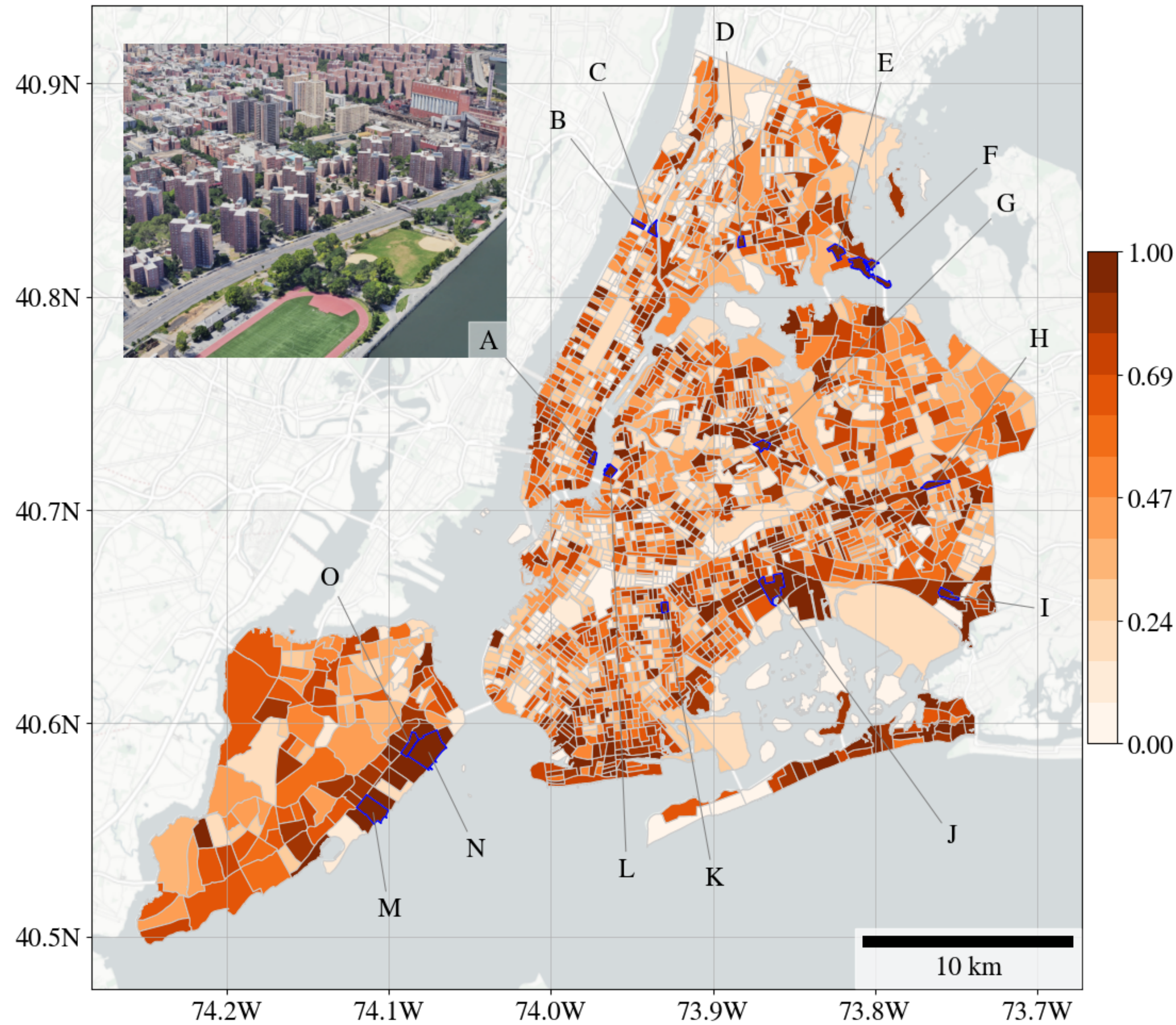

Fig. 6. Values of the prioritization index I across NYC census tracts A_i, for $\gamma = 0.50$. The three tracts from each borough with the highest $I(A_i)$ values are highlighted and labeled with letters A to O. The overlaid image highlights the Census tract labeled as **A**, which encompasses Riis Houses, a residential complex of 1191 units dating back to 1949, situated within the 100-year storm surge flood plain. This tract, known for its high social vulnerability (91$^{\text{st}}$ percentile), also includes the renovated East Side Park, a key green infrastructure project aimed at enhancing flood resiliency.

substantial subway hub (annual AAR at risk of 345,000 passengers), and has a high CDC social vulnerability index (exceeding the 90$^{\text{th}}$ percentile). Sensors could be deployed in this census tract to enable quick decision making on subway closures and the rerouting of vehicular traffic during flood events. In addition, socially vulnerable residents of this tract could leverage the sensor data to advocate for enhanced resilience measures by the city.

Another example is Springfield Gardens in southeastern Queens, labeled ***I*** in Figure 6, frequently cited by the media for its susceptibility to flooding (Costella 2010; Bisram 2022). This area hosts the 146$^{\text{th}}$ Avenue electricity substation and 191 pre-1961 residential buildings in flood-prone zones. It ranks above the 98$^{\text{th}}$ percentile on the Environmental Justice Index for PM 2.5, air toxic cancer risk, and the presence of Underground Storage Tanks. Furthermore, it has only 0.03 human service centers per 1,000 residents – markedly below the city average of 0.18. The disparity between the high number of tax lots in flood-prone areas (191) and the relatively few flood-related 311 reports (29 over 13 years) highlights this community's possible underuse of the 311 reporting system or that the worst floods are yet to happen. Deploying flood sensors could enhance real-time monitoring at critical infrastructure like the electricity substation and provide accurate flood data for older residential buildings. Using sensor data could also address the high social vulnerability of the community by informing targeted resilience measures.

The Use-Case Metric v_7, representing the number of New York State classified environmental remediation sites, is referenced only once in Table 6. The specific location, designated as ***L*** in Figure 6, is situated in the Williamsburg neighborhood of Brooklyn. This area includes two environmental remediation sites contaminated with substances like toluene, ethylbenzene, xylene, and acetone. These chemicals are typical pollutants that can impact soil and groundwater quality and pose risks to human health and the environment. In the event of flooding, these substances could disperse, highlighting the need for sensor monitoring to aid in planning remediation activities.

The same census tract also has a low floor area of public schools per capita (metric v_{10}), approximately 0.75 m^2 per person, which is below the 20th percentile for the city. Tracts with greater public school space per person are less likely to experience educational disruptions, as larger facilities can better absorb impacts and serve as emergency shelters during natural disasters. Conversely, tracts with lower school space can experience additional social vulnerability.

Lastly, we note that two Use-Case Metrics consistently appear across nearly all highlighted Census tracts in Table 6: v_2 (Number of residential units in pre-1961 buildings) and v_3 (Annual Average Daily Vehicular Traffic). This outcome is expected, as buildings and roads are ubiquitous in an urban context.

SUMMARY AND CONCLUSIONS

This study proposes a framework to guide the deployment of hyper-local, real-time flood sensor networks in urban areas, adopting a unique risk-informed, end-user-oriented approach. The framework is composed of three stages. The first stage involves stakeholder elicitation, where various strategically selected stakeholders (e.g., city agencies, researchers, engineering consultants, insurers, and residents) provide feedback on how they might use the sensor data and which corresponding metrics should be leveraged to determine where to deploy the sensors. The metrics gathered from stakeholders fall into two categories: Use-Case Metrics and Social Vulnerability Metrics. The former includes metrics directly linked to specific sensor data applications, such as monitoring vehicular traffic to safeguard transportation infrastructure during floods. The latter pertains to attributes that heighten community vulnerability to natural hazards (e.g., income levels). The second stage integrates these metrics in a flood risk quantification process, using probabilistic risk analysis to combine data on each metric with flood hazard information. Stage three involves the Analytical Hierarchical Process to determine stakeholder preferences for the individual metrics, which are used to combine the metrics into a single index that identifies areas to be prioritized in terms of sensor deployment.

A case study demonstration of the framework was conducted for New York City (NYC), focusing on a new street-level, real-time flood monitoring network. We engaged with key NYC stakeholders across three main categories: government agencies (including emergency responders and public infrastructure managers), research institutions, and the private sector (engineering consultants and insurers). Stakeholders identified 32 possible uses for flood sensor data that we classified into four main categories: emergency response and recovery planning, infrastructure management, risk awareness increase, and flood hazard characterization. An important insight from this feedback is that real-time sensor data has the potential to inform flood risk management decision-making across multiple timescales; it can be used during the emergency phase (e.g., to send early warnings to residents), in the aftermath of an event (e.g., to direct relief operations to the most affected areas), and in the longer term (e.g., for infrastructure planning activities).

The stakeholders then defined 22 Use-Case Metrics, each linked to one or more previously identified uses. Infrastructure management and flood hazard characterization emerged as primary themes among these metrics, reflecting the strong representation of city officials and researchers in our elicitation process. We also observed that the Use-Case Metrics reflected the three core elements of a risk-analysis framework: hazard, exposure, and vulnerability. For instance, the "Historical number of flood-related emergency response incidents" metric pertains to hazard whereas "Number of basement dwellings" primarily corresponds to vulnerability. Other Use-Case Metrics encompass many other risk-analysis elements, e.g., “Historical number of flood insurance claims.”. The stakeholders further identified 35 Social Vulnerability Metrics. These metrics predominantly addressed socioeconomic and demographic factors similar (or equivalent) to established indexes such as the Social Vulnerability Index.

Our proposed index revealed that areas that could be prioritized for sensor deployment in NYC are located in both inland and coastal regions. Furthermore, metrics that exhibit consistently large values across census tracts with the highest priority include “Number of residential units in pre-1961 buildings” and “Annual Average Daily Traffic for vehicular traffic along roads and highways”. This finding is expected, as buildings and roads constitute the majority of the urban environment.

Our case study was not designed to provide a definitive list of NYC areas to be prioritized in terms of flood sensor deployment. Instead, it serves two important alternative purposes: first, it provides a practical demonstration of the proposed framework, and second, it identifies an initial set of stakeholders, use cases, and metrics that can improve current flood sensor deployment strategies. Future applications can strengthen our framework’s application case study by including resident representatives and more a balanced distribution of participants across other stakeholder categories. Despite this limitation, our case study underlines the potential value that this framework could bring to the increasingly prevalent challenge of flood risk management decision-making.

ACKNOWLEDGEMENTS

The authors are thankful for the financial support provided by the NYU Tandon School of

Engineering Fellowship and NYU C2SMART (Grant No. 69A3551747119). We are also thankful to all stakeholders who participated in our workshop and to multiple FloodNet project members who offered invaluable feedback.

REFERENCES

“1961 New York City Zoning Resolution.” *The New York Preservation Archive Project*, <https://www.nypap.org/preservation-history/1961-new-york-city-zoning-resolution/>.

(2023). “Community flood watch project, <https://srijb.org/jbfloodwatch/>.

(2023). “First street foundation, <https://firststreet.org/>.

Alipour, A., Ahmadalipour, A., and Moradkhani, H. (2020). “Assessing flash flood hazard and damages in the southeast United States.” *Journal of Flood Risk Management*, 13(2), e12605 _eprint: https://onlinelibrary.wiley.com/doi/pdf/10.1111/jfr3.12605.

Arora, P. and Ceferino, L. (2023a). “Could rooftop solar panels and storage have enhanced the electricity resilience during Hurricane Isaias (2020)?.” *ICASP 14 Proceedings*.

Arora, P. and Ceferino, L. (2023b). “Probabilistic and machine learning methods for uncertainty quantification in power outage prediction due to extreme events.” *Natural Hazards and Earth System Sciences*, 23(5), 1665–1683 Publisher: Copernicus GmbH.

Arora, P. and Ceferino, L. (2024). “A Quasi-Binomial Regression Model for Hurricane-Induced Power Outages during Early Warning.” *ASCE-ASME Journal of Risk and Uncertainty in Engineering Systems, Part A: Civil Engineering*, 10(2), 04024027.

Avraam, C., Ceferino, L., and Dvorkin, Y. (2023). “Operational and economy-wide impacts of compound cyber-attacks and extreme weather events on electric power networks.” *Applied Energy*, 349, 121577.

Bhatt, C. M. and Srinivasa Rao, G. (2018). “HAND (height above nearest drainage) tool and satellite-based geospatial analysis of Hyderabad (India) urban floods, September 2016.” *Arabian Journal of Geosciences*, 11(19), 600.

Bisram, J. (2022). “Residents of queens communities of springfield gardens and rosedale dealing with flooded basements.” *CBS News New York*.

Blázquez, L., García, J. A., and Bodoque, J. M. (2021). “Stakeholder analysis: Mapping the river networks for integrated flood risk management.” *Environmental Science & Policy*, 124, 506–516.

Catalano de Sousa, M. R., Montalto, F. A., and Gurian, P. (2016). “Evaluating Green Infrastructure Stormwater Capture Performance under Extreme Precipitation.” *Journal of Extreme Events*, 03(02), 1650006 Publisher: World Scientific Publishing Co.

Chambers, R. (2002). *Participatory workshops: A sourcebook of 21 sets of ideas and activities*. Routledge, 1 edition, <https://doi.org/10.4324/9781849772136>.

Chang, H., Yu, Z., Yu, Z., and Guo, B. (2019). “Selecting Sensing Location Leveraging Spatial and Cross-Domain Correlations.” *2019 IEEE SmartWorld, Ubiquitous Intelligence & Computing, Advanced & Trusted Computing, Scalable Computing & Communications, Cloud & Big Data Computing, Internet of People and Smart City Innovation (SmartWorld/SCALCOM/UIC/ATC/CBDCom/IOP/SCI)*, 661–666 (August).

Chawla, I., Karthikeyan, L., and Mishra, A. K. (2020). “A review of remote sensing applications for water security: Quantity, quality, and extremes.” *Journal of Hydrology*, 585, 124826.

Chen, M., Li, Z., Gao, S., Luo, X., Wing, O. E. J., Shen, X., Gourley, J. J., Kolar, R. L., and Hong, Y. (2021). “A Comprehensive Flood Inundation Mapping for Hurricane Harvey Using an Integrated Hydrological and Hydraulic Model.” *Journal of Hydrometeorology*, 22(7), 1713–1726 Publisher: American Meteorological Society Section: Journal of Hydrometeorology.

City of New York (2023). “NYC open data, <https://opendata.cityofnewyork.us/>.

City of San Francisco (2023). “DataSF - open data, <https://data.sfgov.org/>.

Costella, A. (2010). “Flooding devastates springfield gardens.” *Queens Chronicle*.

Cremen, G. and Galasso, C. (2021). “A decision-making methodology for risk-informed earthquake early warning.” *Computer-Aided Civil and Infrastructure Engineering*, 36(6), 747–761 _eprint: https://onlinelibrary.wiley.com/doi/pdf/10.1111/mice.12670.

Cremen, G., Galasso, C., and Zuccolo, E. (2022). “Investigating the potential effectiveness of earthquake early warning across Europe.” *Nature Communications*, 13(1), 639 Publisher: Nature Publishing Group.

Culligan, P. J. (2019). "Green infrastructure and urban sustainability: A discussion of recent advances and future challenges based on multiyear observations in New York City." *Science and Technology for the Built Environment*, 25(9), 1113–1120 Publisher: Taylor & Francis _eprint: https://doi.org/10.1080/23744731.2019.1629243.

Cutter, S. L., Burton, C. G., and Emrich, C. T. (2010). "Disaster Resilience Indicators for Benchmarking Baseline Conditions." *Journal of Homeland Security and Emergency Management*, 7(1) Publisher: De Gruyter.

Daniel, L., Mazumder, R. K., Enderami, S. A., Sutley, E. J., and Lequesne, R. D. (2022). "Community Capitals Framework for Linking Buildings and Organizations for Enhancing Community Resilience through the Built Environment." *Journal of Infrastructure Systems*, 28(1), 04021053 tex.copyright: © 2021 American Society of Civil Engineers.

Davenport, F. V., Burke, M., and Diffenbaugh, N. S. (2021). "Contribution of historical precipitation change to US flood damages." *Proceedings of the National Academy of Sciences*, 118(4), e2017524118 Publisher: Proceedings of the National Academy of Sciences.

Department for International Development (2002). "Tools for development: A handbook for those engaged in development activity." *manual*, Performance and Effectiveness Department, Department for International Development, <https://www.gov.uk/government/organisations/department-for-international-development> (September).

Dow, K. and Cutter, S. L. (2006). "Crying Wolf: Repeat Responses to Hurricane Evacuation Orders." *Hazards Vulnerability and Environmental Justice*, Routledge. Num Pages: 18.

Du, W., Xing, Z., Li, M., He, B., Chua, L. H. C., and Miao, H. (2014). "Optimal sensor placement and measurement of wind for water quality studies in urban reservoirs." *IPSN-14 Proceedings of the 13th International Symposium on Information Processing in Sensor Networks*, 167–178 (April).

Englund, M., Vieira Passos, M., André, K., Gerger Swartling, , Segnestam, L., and Barquet, K. (2023). "Constructing a social vulnerability index for flooding: insights from a municipality in

Sweden." *Frontiers in Climate*, 5 Publisher: Frontiers.

(EPA), U. E. P. A. (2023). "EJScreen technical documentation." *Technical report*, U.S. Environmental Protection Agency.

Finch, C., Emrich, C. T., and Cutter, S. L. (2010). "Disaster disparities and differential recovery in New Orleans." *Population and Environment*, 31(4), 179–202.

Flanagan, B. E., Gregory, E. W., Hallisey, E. J., Heitgerd, J. L., and Lewis, B. (2011). "A Social Vulnerability Index for Disaster Management." *Journal of Homeland Security and Emergency Management*, 8(1) Publisher: De Gruyter.

FloodNet (2024). "FloodNet NYC, <https://www.floodnet.nyc/>.

Fontainha, T. C., Leiras, A., Bandeira, R. A. d. M., and Scavarda, L. F. (2017). "Public-Private-People Relationship Stakeholder Model for disaster and humanitarian operations." *International Journal of Disaster Risk Reduction*, 22, 371–386.

Garbutt, K., Ellul, C., and Fujiyama, T. (2015). "Mapping social vulnerability to flood hazard in Norfolk, England." *Environmental Hazards*, 14(2), 156–186 Publisher: Taylor & Francis _eprint: https://doi.org/10.1080/17477891.2015.1028018.

Gardner, M., Nichols, E., Stark, N., Lemnitzer, A., and Frost, D. (2023). "Multispectral Imaging for Identification of High-Water Marks in Postdisaster Flood Reconnaissance." *NATURAL HAZARDS REVIEW*, 24(2), 06023002 Num Pages: 9 Place: Reston Publisher: Asce-Amer Soc Civil Engineers Web of Science ID: WOS:000952342200020.

Geberemariam, T. K. (2017). "Post Construction Green Infrastructure Performance Monitoring Parameters and Their Functional Components." *Environments*, 4(1), 2 Number: 1 Publisher: Multidisciplinary Digital Publishing Institute.

Gilmour, J. and Beilin, R. (2007). "Stakeholder mapping for effective risk assessment and communication." *Australian Centre for Excellence in Risk Analysis (ACERA) Project*, 609, 1–52.

Giustarini, L., Hostache, R., Matgen, P., Schumann, G. J.-P., Bates, P. D., and Mason, D. C. (2013). "A Change Detection Approach to Flood Mapping in Urban Areas Using TerraSAR-X." *IEEE Transactions on Geoscience and Remote Sensing*, 51(4), 2417–2430 Conference Name: IEEE

Transactions on Geoscience and Remote Sensing.

Hemming, V., Burgman, M. A., Hanea, A. M., McBride, M. F., and Wintle, B. C. (2018). "A practical guide to structured expert elicitation using the IDEA protocol." *Methods in Ecology and Evolution*, 9(1), 169–180 _eprint: https://onlinelibrary.wiley.com/doi/pdf/10.1111/2041-210X.12857.

International Association for Public Participation (2004). "Public participation toolbox." *manual*, <https://www.iap2.org/>.

Knol, A. B., Slottje, P., van der Sluijs, J. P., and Lebret, E. (2010). "The use of expert elicitation in environmental health impact assessment: a seven step procedure." *Environmental Health*, 9(1), 19.

Krabbenhoft, C. A., Allen, G. H., Lin, P., Godsey, S. E., Allen, D. C., Burrows, R. M., DelVecchia, A. G., Fritz, K. M., Shanafield, M., Burgin, A. J., Zimmer, M. A., Datry, T., Dodds, W. K., Jones, C. N., Mims, M. C., Franklin, C., Hammond, J. C., Zipper, S., Ward, A. S., Costigan, K. H., Beck, H. E., and Olden, J. D. (2022). "Assessing placement bias of the global river gauge network." *Nature Sustainability*, 5(7), 586–592 Publisher: Nature Publishing Group.

Krause, A., Singh, A., and Guestrin, C. (2008). "Near-Optimal Sensor Placements in Gaussian Processes: Theory, Efficient Algorithms and Empirical Studies." *The Journal of Machine Learning Research*, 9, 235–284.

Lee, E. K., Donley, G., Ciesielski, T. H., Gill, I., Yamoah, O., Roche, A., Martinez, R., and Freedman, D. A. (2022). "Health outcomes in redlined versus non-redlined neighborhoods: A systematic review and meta-analysis." *Social Science & Medicine*, 294, 114696.

Lin, X. and Kwon, W. J. (2020). "Application of parametric insurance in principle-compliant and innovative ways." *Risk Management and Insurance Review*, 23(2), 121–150 _eprint: https://onlinelibrary.wiley.com/doi/pdf/10.1111/rmir.12146.

Loftis, D., Forrest, D., Katragadda, S., Spencer, K., Organski, T., Nguyen, C., and Rhee, S. (2018). "StormSense: A New Integrated Network of IoT Water Level Sensors in the Smart Cities of Hampton Roads, VA." *Marine Technology Society Journal*, 52.

Long, C. (2017). “Public Schools Offer Shelter from the Storm | NEA.” *NEA Today Magazines - National Education Association*.

Mason, D. C., Davenport, I. J., Neal, J. C., Schumann, G. J.-P., and Bates, P. D. (2012). “Near Real-Time Flood Detection in Urban and Rural Areas Using High-Resolution Synthetic Aperture Radar Images.” *IEEE Transactions on Geoscience and Remote Sensing*, 50(8), 3041–3052 Conference Name: IEEE Transactions on Geoscience and Remote Sensing.

Mojtahedi, M. and Oo, B. L. (2017). “Critical attributes for proactive engagement of stakeholders in disaster risk management.” *International Journal of Disaster Risk Reduction*, 21, 35–43.

Munawar, H. S., Hammad, A. W. A., and Waller, S. T. (2022). “Remote Sensing Methods for Flood Prediction: A Review.” *Sensors*, 22(3), 960 Number: 3 Publisher: Multidisciplinary Digital Publishing Institute.

Mydlarz, C., Sai Venkat Challagonda, P., Steers, B., Rucker, J., Brain, T., Branco, B., Burnett, H. E., Kaur, A., Fischman, R., Graziano, K., Krueger, K., Hénaff, E., Ignace, V., Jozwiak, E., Palchuri, J., Pierone, P., Rothman, P., Toledo-Crow, R., and Silverman, A. I. (2024). “FloodNet: Low-Cost Ultrasonic Sensors for Real-Time Measurement of Hyperlocal, Street-Level Floods in New York City.” *Water Resources Research*, 60(5), e2023WR036806 _eprint: https://onlinelibrary.wiley.com/doi/pdf/10.1029/2023WR036806.

Negri, R., Fernandez, M., Tsai, J., Tan, B., and Ceferino, L. (2023). “Investigating the Use of Citizen-Science Data as a Proxy for Flood Risk Assessment in New York City (July).

New York City Government (2023). “Hurricane ida action plan substantial amendment 1, <https://www.nyc.gov/assets/cdbgdr/documents/amendments/Ida$_{A}mendments/2_{N}YC_{H}urricane_{I}da_{A}ction_{P}la$

Newman, A. (2021). “What we know about the people who died in the flooding..” *The New York Times*.

NYC Mayor’s Office of Resiliency (2021). “New york city stormwater resiliency plan.” *Report no.*, <https://www1.nyc.gov/assets/orr/pdf/publications/stormwater-resiliency-plan.pdf>.

NYCDCP (2023). “NYC Equitable Development Data Explorer, <https://equitableexplorer.planninglabs.nyc> (May).

Patrick, L., Solecki, W., Gornitz, V., Orton, P., and Blumberg, A. (2019). "New York City Panel on Climate Change 2019 Report Chapter 5: Mapping Climate Risk." *Annals of the New York Academy of Sciences*, 1439(1), 115–125 _eprint: https://onlinelibrary.wiley.com/doi/pdf/10.1111/nyas.14015.

Plumer, B. (2021). "New Yorkers Got Record Rain, and a Warning: Storms Are Packing More Punch." *The New York Times*.

Pouloudi, A. and Whitley, E. A. (1997). "Stakeholder identification in inter-organizational systems: gaining insights for drug use management systems." *European Journal of Information Systems*, 6(1), 1–14 Publisher: Taylor & Francis _eprint: https://doi.org/10.1057/palgrave.ejis.3000252.

Rabinovici, S., Mieler, M., Miranda, E., Mitrani-Reiser, J., Stewart, J. P., Tremayne, H., Ortiz-Millan, M., and Cullman, C. (2022). "Organizing post-earthquake reconnaissance to optimize impact: Workshop summary and outcomes report." *EERI learning from earthquakes program report*, Earthquake Engineering Research Institute, Oakland, California (November).

Rajapaksa, D., Wilson, C., Managi, S., Hoang, V., and Lee, B. (2016). "Flood Risk Information, Actual Floods and Property Values: A Quasi-Experimental Analysis." *Economic Record*, 92(S1), 52–67 _eprint: https://onlinelibrary.wiley.com/doi/pdf/10.1111/1475-4932.12257.

Reed, M. S. (2008). "Stakeholder participation for environmental management: A literature review." *Biological Conservation*, 141(10), 2417–2431.

Rosenzweig, C., Solecki, W., College, H., Blake, R., Bowman, M., Gornitz, V., Jacob, K., Kinney, P., Kunreuther, H., Kushnir, Y., Leichenko, R., Lin, N., Nordenson, G., Oppenheimer, M., Yohe, G., Horton, R., Lead, C., Patrick, L., Bader, D., and Ali, S. (2013). "New York City Panel on Climate Change (NPCC2)." *Report no.*, <https://data.cityofnewyork.us/api/assets/581A4132-3843-4C3B-8B80-D268257AC778?download=true>.

Saaty, R. W. (1987). "The analytic hierarchy process—what it is and how it is used." *Mathematical Modelling*, 9(3), 161–176 Number: 3.

Saisana, M., Saltelli, A., and Tarantola, S. (2005). "Uncertainty and Sensitivity Analysis Techniques as Tools for the Quality Assessment of Composite Indicators." *Journal of the Royal Statistical Society Series A: Statistics in Society*, 168(2), 307–323.

Sanders, B. F., Schubert, J. E., Kahl, D. T., Mach, K. J., Brady, D., AghaKouchak, A., Forman, F., Matthew, R. A., Ulibarri, N., and Davis, S. J. (2023). “Large and inequitable flood risks in Los Angeles, California.” *Nature Sustainability*, 6(1), 47–57 Number: 1 Publisher: Nature Publishing Group.

Sarchani, S., Seiradakis, K., Coulibaly, P., and Tsanis, I. (2020). “Flood Inundation Mapping in an Ungauged Basin.” *Water*, 12(6), 1532 Number: 6 Publisher: Multidisciplinary Digital Publishing Institute.

School, U. G. S. U. W. S. (2018). “High-water marks and flooding, <https://www.usgs.gov/special-topics/water-science-school/science/high-water-marks-and-flooding: :text=At

Scolobig, A., Komendantova, N., Patt, A., Vinchon, C., Monfort-Climent, D., Begoubou-Valerius, M., Gasparini, P., and Di Ruocco, A. (2014). “Multi-risk governance for natural hazards in Naples and Guadeloupe.” *Natural Hazards*, 73(3), 1523–1545.

Silverman, A. I., Brain, T., Branco, B., Challagonda, P. s. v., Choi, P., Fischman, R., Graziano, K., Hénaff, E., Mydlarz, C., Rothman, P., and Toledo-Crow, R. (2022). “Making waves: Uses of real-time, hyperlocal flood sensor data for emergency management, resiliency planning, and flood impact mitigation.” *Water Research*, 220, 118648.

Sun, C., Li, V. O., and Lam, J. C. (2018). “Optimal Citizen-Centric Sensor Placement for Citywide Environmental Monitoring - A Submodular Approach.” *2018 IEEE International Conference on Sensing, Communication and Networking (SECON Workshops)*, 1–4 (June). ISSN: 2155-5494.

Sun, C., Li, V. O. K., Lam, J. C. K., and Leslie, I. (2019). “Optimal Citizen-Centric Sensor Placement for Air Quality Monitoring: A Case Study of City of Cambridge, the United Kingdom.” *IEEE Access*, 7, 47390–47400 Conference Name: IEEE Access.

Tien, I., Lozano, J.-M., and Chavan, A. (2023). “Locating real-time water level sensors in coastal communities to assess flood risk by optimizing across multiple objectives.” *Communications Earth & Environment*, 4(1), 1–12 Publisher: Nature Publishing Group.

United States Bureau of the Census (1994). “Geographic areas reference manual.” *manual*, U.S. Department of Commerce, Economics and Statistics Administration, Bureau of the Census, Washington, D.C., <https://purl.fdlp.gov/GPO/LPS53335>. Type: Handbooks and manuals tex.additionalform: Also available via Internet from U.S. Dept. of Census website tex.bibnote: Includes bibliographical references tex.description: 1 volume (various pagings) : illustrations, maps tex.generalnote: Shipping list no.: 94-0400-P tex.howpublished: Online tex.oclc: 31785521 tex.subject: United States – Census – Methodology; Census districts – United States – Handbooks, manuals, etc.; United States – Population – History; Geographical location codes – Handbooks, manuals, etc.

Waraich, I. (2023). "Here's how special sensors along NYC streets are monitoring flood events across the 5 boroughs." *silive* Section: News.

Wates, N. (2014). *The Community Planning Handbook: How People Can Shape Their Cities, Towns and Villages in Any Part of the World*. Routledge (April) Google-Books-ID: xrVEAwAAQBAJ.

Webster, S. E., Donovan, E. C., Chudoba, E., Hesed, C. D. M., Paolisso, M., and Dennison, W. C. (2022). "Identifying and harmonizing the priorities of stakeholders in the Chesapeake Bay environmental monitoring community." *CURRENT RESEARCH IN ENVIRONMENTAL SUSTAINABILITY*, 4, 100155 Num Pages: 13 Place: Amsterdam Publisher: Elsevier Web of Science ID: WOS:000905612500013.

Wikipedia contributors (2023). "3-1-1 — Wikipedia, the free encyclopedia, <https://en.wikipedia.org/wiki/3-1-1>.

Wing, O., Quinn, N., Uhe, P., Savage, J., Sampson, C., Addor, N., Lord, N., Collings, T., Hatchard, S., Hoch, J., Smith, A., Cooper, A., Bates, J., Wilkinson, H., Himsworth, S., Probyn, I., Haigh, I., Neal, J., and Bates, P. (2023). "A 30 m resolution global fluvial–pluvial–coastal flood inundation model for any climate scenario." *Report No. EGU23-6383*, Copernicus Meetings, <https://meetingorganizer.copernicus.org/EGU23/EGU23-6383.html> (February). Conference Name: EGU23.

Wu, X., Liu, M., and Wu, Y. (2012). "In-situ soil moisture sensing: Optimal sensor placement and field estimation." *ACM Transactions on Sensor Networks*, 8(4), 33:1–33:30.

Yu, J. and Leung, M.-y. (2018). "Structural Stakeholder Model in Public Engagement for Construction

Development Projects." *Journal of Construction Engineering and Management*, 144(6), 04018046 Publisher: American Society of Civil Engineers.

Yu, Z., Chang, H., Yu, Z., Guo, B., and Shi, R. (2022). "Location Selection for Air Quality Monitoring With Consideration of Limited Budget and Estimation Error." *IEEE Transactions on Mobile Computing*, 21(11), 4025–4037 Conference Name: IEEE Transactions on Mobile Computing.